Airway epithelial tight junctions and binding and cytotoxicity of *Pseudomonas aeruginosa*

ALFRED LEE,[1] DAR CHOW,[1] BRIAN HAUS,[1] WANRU TSENG,[1] DAVID EVANS,[2]
SUZANNE FLEISZIG,[2] GRISCHA CHANDY,[1] AND TERRY MACHEN[1]
[1]*Department of Molecular and Cell Biology, University of California, Berkeley 94720-3200;
and* [2]*School of Optometry, University of California, Berkeley, California 94720-2020*

Lee, Alfred, Dar Chow, Brian Haus, Wanru Tseng, David Evans, Suzanne Fleiszig, Grischa Chandy, and Terry Machen. Airway epithelial tight junctions and binding and cytotoxicity of *Pseudomonas aeruginosa*. *Am. J. Physiol.* 277 (*Lung Cell. Mol. Physiol.* 21): L204–L217, 1999.— The role of tight junctions in the binding and cytoxicity of *Pseudomonas aeruginosa* to apical or basolateral membranes of lung airway epithelial cells was tested with fluorescence microscopy on living cells. Binding of noncytotoxic *P. aeruginosa* strain O1 was assessed with *P. aeruginosa* that expressed green fluorescent protein. Binding of cytotoxic *P. aeruginosa* strain 6206 was assessed with FITC-labeled *P. aeruginosa*; cytotoxicity was determined from nuclear uptake of the impermeant dye propidium iodide. The role of direct contact of *P. aeruginosa* to epithelial cells was tested with filters with small (0.45-µm) or large (2.0-µm) pores. High transepithelial resistance (R_t) Calu-3 and cultured bovine tracheal monolayers ($R_t > 1,000 \ \Omega \cdot cm^2$) bound *P. aeruginosa* very infrequently (<1 *P. aeruginosa*/100 cells) at the apical membrane, but *P. aeruginosa* bound frequently to cells near "free edges" at holes, wounds, islands, and perimeters; cytotoxicity required direct interaction with basolateral membranes. Wounded high R_t epithelia showed increased *P. aeruginosa* binding and cytotoxicity at the free edges because basolateral membranes were accessible to *P. aeruginosa*, and dead and living cells near the wound bound *P. aeruginosa* similarly. Compared with high R_t epithelia, low R_t CFT1 ($R_t = 100$–$200 \ \Omega \cdot cm^2$) and EGTA-treated Calu-3 monolayers were 25 times more susceptible to *P. aeruginosa* binding throughout the monolayer. Cytotoxicity to CFT1 cells (throughout the confluent monolayer, not only at the free edge) occurred after a shorter delay (0.25 vs. 2.0 h) and then five times faster than to Calu-3 cells, indicating that the time course of *P. aeruginosa* cytotoxicity may be limited by the rate of gaining access through tight junctions and that this occurred faster in low R_t than in high R_t airway epithelia. Cytotoxicity appeared to occur in a sequential process that led first to a loss of fura 2 and a later uptake of propidium iodide. *P. aeruginosa* bound three times more frequently to regions between cells (tight junctions?) than to cell membranes of low R_t CFT1 cells.

epithelial cells; cystic fibrosis; cystic fibrosis transmembrane conductance regulator; green fluorescence protein; Calu-3 cells; trachea; epithelial polarity

---

ALTHOUGH IT IS COMMONLY ASSUMED that the critical first steps in bacterial-induced pathogenesis in cystic fibrosis (CF) involve binding and subsequent direct and indirect cytotoxic effects of *Pseudomonas aeruginosa* to airway cells, the respective roles of bacterial and host factors that contribute to the pathogenesis of *P. aeruginosa* airway infection in CF remain controversial. One area of controversy has been the identity of *P. aeruginosa* receptors on the apical and/or basolateral membranes of airway epithelial cells. Imundo et al. (19) showed two- to threefold greater binding of *P. aeruginosa* to CF- versus CF transmembrane conductance regulator (CFTR)-corrected epithelial cell lines (also see Refs. 30, 36). Because antibodies against asialo-G_{M1} reduced *P. aeruginosa* binding and asialo-G_{M1} appeared from immunofluorescence to be on the apical membrane, it was proposed that *P. aeruginosa* bound to this glycolipid in the apical membranes of wild-type (WT) and especially CF airway epithelial cells (19; also see Refs. 2, 9, 15, 22, 30, 32, 36). Consistent with some aspects of these findings, De Bentzmann and colleagues (2, 3) found that *P. aeruginosa* bound mainly to the dorsal, apparently apical, membranes of tracheal cells at the edges of wounds (also see Refs. 10, 32, 37) and that binding was blocked by anti-asialo-G_{M1} antibodies (2).

In contrast, Pier and colleagues (25–27) showed that *P. aeruginosa* bound and were taken up to a greater extent by cells expressing WT CFTR than cells expressing either no CFTR or ΔF508 CFTR. They also showed that *P. aeruginosa* invasion of epithelial cells was increased during incubation of CF epithelial cells at 26°C (to increase expression of ΔF508 CFTR on the apical membrane), whereas *P. aeruginosa* invasion was blocked by an antibody against CFTR (26, 27) and electron microscopy showed that *P. aeruginosa* bound to CFTR (25). To explain their data, Pier et al. (25) proposed that *P. aeruginosa* bound to the membranes of airway cells and that this binding of *P. aeruginosa* recruited CFTR to the membrane. CFTR then served as an uptake mechanism for *P. aeruginosa*. Because CFTR is located at the apical membrane of airway epithelial cells, it was reasonable to assume that this binding and uptake of *P. aeruginosa* was similarly occurring at the apical membrane.

In contrast, other work has indicated that *P. aeruginosa* bound and elicited cytotoxicity by interacting with the basolateral membranes of epithelial cells. Thus there was little binding when *P. aeruginosa* were added to the apical sides of intact epithelial cell layers, and *P. aeruginosa* binding increased after tissue injury or other treatment that allowed *P. aeruginosa* access to the basolateral membrane (e.g., Refs. 28, 32). Fleiszig et al. (10) recently found that *P. aeruginosa* binding and/or cytotoxicity increased 10- to 300-fold when basolateral membranes of well-polarized tracheal, na-

sal, Madin-Darby canine kidney (MDCK), and corneal cells were exposed by disrupting tight junctions (EGTA treatment), by growing cells in a low-calcium concentration (prevents tight junction formation), or by using subconfluent cells (10). In addition, scratch wounding of corneal epithelial cells leads to 10- to 100-fold increases in *P. aeruginosa* adherence and rendered the cornea susceptible to infection (14, 28). Apical addition of *P. aeruginosa* to the apical surfaces of MDCK and corneal epithelial cells induced cytotoxicity as expanding foci of dying cells, indicating that once cytotoxicity was induced, cells adjacent to dying cells were affected (1, 14). Also, direct contact of whole, viable *P. aeruginosa* was required for cytotoxicity to MDCK (1) and corneal (14) epithelial cells, and *P. aeruginosa* were found beneath affected cells but not under viable epithelial cells (1; also see Ref. 10). The recently discovered protein ExoU (9; also see Refs. 12, 20), which is required for the acute (within 3 h) cytotoxicity of *P. aeruginosa*, is likely to be secreted by a type III mechanism (9, 34) that requires direct contact between *P. aeruginosa* and epithelial cells. Accordingly, it has been proposed that the maintenance of normal cell polarity is a defense against infection (10).

However, there have been no direct observations of *P. aeruginosa* binding to living airway epithelial cells. In addition, the question of polarized cytotoxicity through direct contact of *P. aeruginosa* with either the apical or basolateral membrane of airway epithelial cells has also not been definitively answered; previous experiments (1) showed that 0.45-µm-pore filters prevented cytotoxicity to MDCK cells, but it was not determined whether critical contact of *P. aeruginosa* was with the apical or basolateral membrane. It is important to note in this regard that MDCK cells are a low-resistance epithelium [transepithelial resistance (R_t) = 100 $\Omega \cdot$cm^2], whereas most airway epithelia exhibit R_t > 600 $\Omega \cdot$cm^2. It is possible that these different R_t values could be crucial in the normal pathophysiological reactions occurring between *P. aeruginosa* and epithelial cells. For example, if cytotoxicity occurs from the basolateral surface, then apically applied *P. aeruginosa* will likely first have to traverse the tight junctions to gain access to the basolateral membranes, and the tighter junctions of airway epithelia could therefore lead to quite different pathophysiological circumstances compared with MDCK (renal proximal tubule) cells.

Given the contradictory findings regarding the interactions of *P. aeruginosa* with different epithelial cells and the potentially different pathophysiological reactions that could occur in airway versus MDCK and other epithelial cells, we made a direct determination (fluorescence and confocal microscopy) of the binding and cytotoxicity of *P. aeruginosa* to two human, CFTR-expressing airway epithelial cell lines, one with high R_t (>1,000 $\Omega \cdot$cm^2) and the other with low R_t (<200 $\Omega \cdot$cm^2). We also used primary cultures of bovine tracheal epithelial cell monolayers for comparison.

METHODS AND MATERIALS

Cultured Calu-3 epithelial cells. Calu-3 cells of human pulmonary adenocarcinoma origin (kindly provided by Dr. Jonathan H. Widdicombe, Children's Hospital, Oakland, CA) were used because they are a tracheal, serouslike cell line with high resistance (1,000–2,000 $\Omega \cdot$cm^2) that grows to confluence, and the cells express functional, cAMP- and ATP-stimulated CFTR in their apical membranes in large amounts (17). Thus these cells formed functional tight junctions, were well polarized and physiologically responsive, and had CFTR in their apical membranes (17, 31). The cells were maintained in Dulbecco's modified Eagle's medium (Sigma, St. Louis, MO) supplemented with 10% fetal calf serum (University of California, San Francisco Cell Culture) in a humidifed 5% CO_2-95% air atmosphere. Cells grown to 80% confluence were trypsinized with 0.25% trypsin-0.1% EGTA solution for 5–15 min. Cells were passaged at a 1:5 dilution, and the remaining cell suspension was seeded directly onto 25-mm cover glasses or permeable filter supports (0.45- or 1.0-µm pore size; Falcon, Becton Dickinson, Franklin Lakes, NJ) at a density of 10^6 cells/cm^2. Cells grown on cover glasses were then allowed to grow into small islands or to complete confluence. Calu-3 cells grown as islands were used to investigate binding to both "free edges" and confluent regions of the monolayer. Cells grown on filters were monitored for R_t with an epithelial volt-ohmmeter (EVOM, World Precision Instruments), and monolayers were used when R_t was >1,000 $\Omega \cdot$cm^2. In some cases, confluent monolayers on either cover glasses or filters were mechanically wounded with a sterile filter tip, and the cells were then placed back into the incubator for 2–24 h to allow the wound to heal before experimentation.

Cultured bovine tracheal epithelial cells. The method was based on the approaches of Wu et al. (33) and Kondo et al. (21), and the cells were prepared in the laboratory of J. Widdicombe. Briefly, bovine tracheae were obtained from the slaughterhouse, and the cells were isolated from the underlying muscle and connective tissue layers by enzyme treatment; after centrifugation, the cells were plated on collagen-coated Falcon filters (0.45-µm pore diameter) and then cultured with an air interface on the apical side. These cell cultures are a mixed population that come predominantly from surface-ciliated, nonciliated, and mucus-secreting cells. After 7–10 days, R_t, measured with an epithelial volt-ohmmeter, reached 1,000–2,000 $\Omega \cdot$cm^2. Only monolayers that had R_t > 1,000 $\Omega \cdot$cm^2 were used for these studies.

Cultured CFTR-corrected CF tracheal epithelial cells. Immortalized CF tracheal epithelial cells that express retrovirally mediated normal CFTR cDNA (clone CFT1-Exp1-C1) were used (24). These cells are homozygous for the ∆F508 mutation and also express WT CFTR. We refer to these cells as CFT1 cells. The CFT1 cells were cultured in hormone-supplemented Ham's F-12 medium (GIBCO BRL, Life Technologies) containing 100 U/ml of penicillin, 100 mg/ml of streptomycin, and 4 mM glutamine (supplements: 5 µg/ml of insulin, 3.7 ng/ml of epidermal growth factor, 3 × 10^{-8} M triiodothyronine, 10^{-6} M hydrocortisone, and 5 µg/ml of transferrin). Cells were passaged at a 1:5 dilution, and the remaining cells were plated onto 0.45-µm-pore filters (Falcon, Becton Dickinson) at a density of 10^6 cells/cm^2. R_t was measured with the volt-ohmmeter, and the monolayers used had R_t = 100–200 $\Omega \cdot$cm^2. As shown previously by Yankaskas et al. (35), CFT1 cells develop vectorial ion transport, and Illek et al. (18) have previously shown they exhibit apical

anion conductance that is identical in properties to CFTR. Thus CFT1 cells express physiological properties consistent with typical tight junctions (albeit with low R_t) and apical-basolateral polarity.

Solutions. Epithelial cells were incubated in a Ringer solution containing (in mM) 135 NaCl, 1.2 MgSO$_4$, 2 CaCl$_2$, 2.4 K$_2$HPO$_4$, 0.6 KH$_2$PO$_4$, 20 HEPES, and 10 glucose (pH 7.4). Fluorescent dyes 2′,7′-bis(2-carboxyethyl)-5(6)-carboxyfluorescein (BCECF)-AM, fura 2-AM, and fura red-AM were prepared as stock solutions in DMSO plus the dispersing agent pluronic F-127. These were added to the cells at a final DMSO concentration of 0.1–0.5%.

P. aeruginosa. *P. aeruginosa* strains 6206 and 103 (PA6206 and PA103, respectively; both cytotoxic strains serogroup O11) and *P. aeruginosa* strain O1 (PAO1) expressing green fluorescent protein (PAO1-GFP; invasive strain serogroup O5; see Ref. 5) were maintained frozen in trypticase soy broth with 10% (vol/vol) glycerol at −70°C. The day before the experiments, *P. aeruginosa* were grown on a trypticase soy agar surface at 37°C overnight and then resuspended in sterile normal Ringer solution to a standardized density of 10^8 colony-forming units (cfu)/ml (0.1 absorbance, 650 nm). Dilutions of this stock solution were then used for subsequent additions to the epithelial cells.

Bright-field and wide-field fluorescence and confocal microscopy of airway epithelial cells and P. aeruginosa. Interactions between epithelial cells and *P. aeruginosa* were observed with both bright-field and fluorescence optics. PAO1-GFP cells were observed with fluorescence. PA6206 cells were also observed with fluorescence after treatment of the bacteria with 1 mg/ml of FITC for 1 h followed by three to six centrifugations and washings to eliminate dye in the solution (see Refs. 4, 6). Cellular patterns of FITC-labeled PA6206 binding were the same as those exhibited by PAO1, and rates of cytotoxicity (see Figs. 9 and 10) induced by PA6206 were the same for control and FITC-labeled bacteria, indicating that FITC labeling had no deleterious effect on the bacteria.

Calu-3, CFT1, and bovine tracheal cells were observed with both Nomarski and fluorescence methods. For fluorescence labeling of the cytosol, cells were incubated with 2–10 μM acetoxymethyl ester (membrane-permeant) version of either BCECF (green), fura 2 (blue), or fura red (red) for 1 h followed by three washes with fresh solution. Treatment of Calu-3 cells with 10 μM probenecid during the loading process was an effective way to reduce the loss of dye, but similar results in terms of *P. aeruginosa*-Calu-3 cell interactions were obtained with or without probenecid during loading. One to ten micromolar propidium iodide (PI) was added to the Ringer solutions to identify dead epithelial cells by staining the nuclei with the dye (red). In Calu-3 cells that had been loaded with either BCECF, fura 2, or fura red, cell death was observed as a loss of cytosolic dye and uptake of PI into the nucleus. Rates of PA6206-induced cytotoxicity were the same for control cells and for cells that had been loaded with fura 2 or BCECF (see Figs. 9–11).

Two approaches were used for observing the interactions between *P. aeruginosa* and epithelial cells. In the first, cells grown on cover glasses were mounted in a chamber that allowed perfusion to maintain the cells viable and could be mounted either right side up or upside down. This chamber was mounted directly on the stage of either an inverted microscope (Zeiss IM35 or Nikon Diaphot) with standard wide-field fluorescence attachments and Nomarski optics or on an upright microscope (Nikon Optiphot) outfitted for confocal microscopy (488-nm laser with filters appropriate for fluorescein and Texas red; Bio-Rad MRC 600). Wide-field fluorescence microscopy was performed with a 75-W xenon light source and either 380 ± 5-, 490 ± 5-, or 530 ± 15-nm excitation and 410 long-pass, 520- to 550-nm band-pass, or 520 or 560 long-pass emission filters. For observing *P. aeruginosa*-epithelial cell interactions on cover glasses, a Nikon oil-immersion lens (1.4 numerical aperture; Neofluar) was used.

Two methods were used for observations of epithelial cells grown on filters. In the first, the filter cup was mounted directly into the chamber, and the fluorescence of Calu-3 cells was observed with one of the inverted microscopes through the filter with a long-working-distance (1.6-mm), water-immersion lens (0.75 numerical aperture; Zeiss). This approach had the advantage that the cells retained their normal polarized orientation, but it had the disadvantage that the optics were compromised. In the second set of experiments, filters were cut from the plastic cups and placed cell side down in the chamber for observation with the inverted microscope. This approach had the advantage of retaining somewhat better optics, although this required cutting the filter from the cup.

Images were recorded with two methods. In one set of experiments, bright-field and wide-field fluorescence images were recorded photographically (35-mm Nikon), and the slides were scanned (Polaroid Sprint Scan 35) and manipulated with Adobe PhotoShop on a Macintosh computer. In another set of experiments, all images were recorded with a Photometrics SenSys charge-coupled device. Digitized confocal images were collected in 0.5-μm steps, stored on the hard disk of a Gateway computer, reconstructed in 2.5-μm projection planes, and displayed with Adobe PhotoShop.

To gain quantitative insights into the specific areas of epithelial cells that bound bacteria, micrographs of monolayers and islands of epithelial cells that showed PAO1-GFP still attached after 1 h of incubation (with 10^7 cfu/ml) and being washed were inspected. For Calu-3 cells, PAO1-GFP cells were bound almost exclusively to cells that were within 70 μm of a free edge. We measured (in both wide-field and confocal micrographs) the linear distances that PAO1-GFP cells were found from random regions of the free edges surrounding Calu-3 islands and adjacent to holes in monolayers, wounded monolayers, and dead cells in wounded monolayers in two to nine different samples. Averages of these 2–9 different random regions were then averaged to obtain an average (±SD) distance (also including range) that PAO1-GFP cells were found away from the free edges of islands, holes in monolayers, wounded monolayers, and dead cells in wounded monolayers for 3–15 different experiments; *n* refers to the number of separate experiments. In addition, the punctate nature of PAO1-GFP made it possible to count the number of PAO1-GFP cells bound (after exposure of 10^6 to 10^7 cfu/ml for 1 h followed by three washes to eliminate loosely adherent bacteria) to the apical and basolateral surfaces of the epithelium with confocal images of the apicalmost section and basalmost regions of both Calu-3 islands and confluent monolayers that had been wounded and then allowed to heal. Bound PAO1-GFP cells were defined as those bacteria that were found within the boundaries of the cell.

For CFT1 cells, binding of *P. aeruginosa* occurred throughout the monolayer and frequently to the tight junctional regions between adjacent cells. To quantitate this aspect of binding, images of PAO1-GFP were overlaid on bright-field images of the epithelial cells. *P. aeruginosa* were categorized as binding to either cells or tight junctions (within 1 μm of distinct tight junctions). We did not count *P. aeruginosa* that bound in the few cases (<10%) where cells were inadequately distinct to tell whether binding was to the cells or junctions.

RESULTS

PAO1-GFP cells bound heterogeneously to basolateral membranes of high R_t Calu-3 cells near free edges. PAO1-GFP cells (10^6 to 10^8 cfu/ml) were added to Calu-3 cells grown on either filters or cover glasses as islands (and not subjected to any mechanical damage) for 1 h and then washed to remove loosely adherent bacteria. Preliminary experiments showed that there was little or no binding of PAO1-GFP cells to confluent regions of Calu-3 cells grown on filters, although there was binding to cells around the extreme perimeter of the filter. We therefore adopted the following approach to test for binding to cells in confluent regions versus at regions that had exposed lateral cell borders. Monolayers were grown as described in *Cultured Calu-3 epithelial cells* and wounded with a pipette tip. The cells were then placed back in the incubator for 1–3 days to allow the monolayer to repair so that there were no dead cells along the edge of the wounded monolayer. This approach led to a filter covered with confluent regions separated by several denuded regions. As shown in Fig. 1, *Aa* and *Ab*, PAO1-GFP cells did not bind to confluent regions of Calu-3 cells grown on filters but only to cells near the free edge. Nearly identical results were found for Calu-3 cells grown on cover glasses (Fig. 1, *Ba* and *Bb*), which had the experimental advantage of permitting bright-field observations of the epithelial cells: PAO1-GFP cells bound to both the glass and the cells with exposed free edges but not to cells that were more than two to three cells from the free edge. These experiments indicated that patterns of PAO1-GFP binding to Calu-3 cells were nearly identical whether the cells were grown on filters or cover glasses.

Similar results were obtained for Calu-3 cells grown as islands on cover glasses with no mechanical perturbation (Fig. 2*A*). PAO1-GFP cells were found an average of 11 μm from the free edges of the islands but no farther than 40 μm from the edges of islands (Table 1). In some experiments, there were small holes in the otherwise confluent monolayer, and PAO1-GFP cells adhered only to cells surrounding these holes (data not shown) an average of 17 μm from the free edges of the holes and no farther than 35 μm (Table 1). The pattern of PAO1-GFP binding to Calu-3 cells was heterogeneous, with some cells binding a few or many bacteria, whereas their neighbors bound none. PAO1-GFP cells often bound in larger numbers to dead Calu-3 cells and to cells near the dead cells (Fig. 3), but there was no preferential binding solely to dead cells. Inspection of regions adjacent to dead cells (within 10 μm) in wounded monolayers showed that PAO1-GFP bound an average of 26 μm from the edges of the wounded monolayers and no farther than 70 μm from the free edge (Table 1). Inspection of the same wounded monolayers showed PAO1-GFP bound an average of 29 μm from the edges of intact cells and no farther than 70 μm from the free edge (Table 1).

Similar experiments were also performed on fura red-loaded confluent islands grown on cover glasses with confocal microscopy. A typical series of 2.5-μm
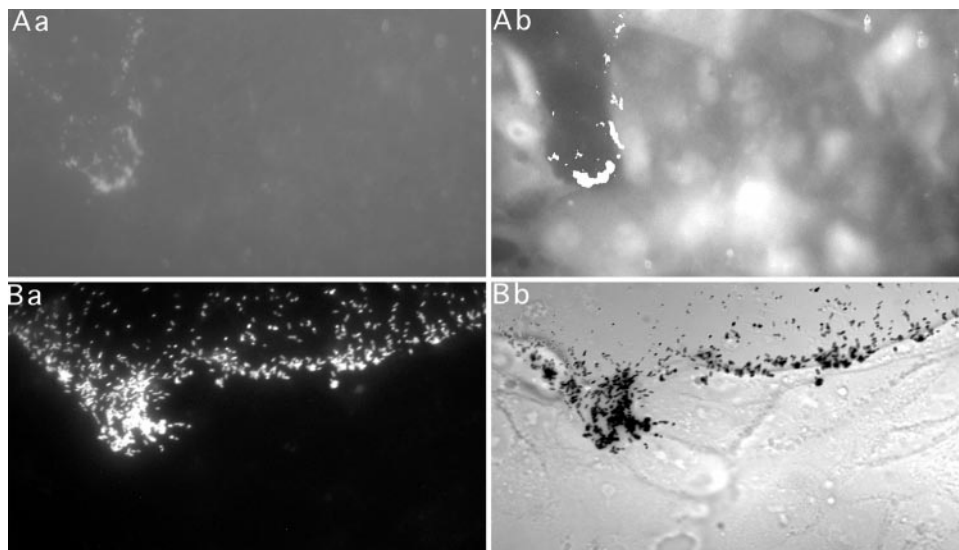

Fig. 1. *Pseudomonas aeruginosa* (PA) strain O1 expressing green fluorescent protein (PAO1-GFP) bound to free edges but not to confluent regions of Calu-3 cells grown either on filters (*A*) to a transepithelial resistance (R_t) > 1,000 Ω·cm² or on cover glasses (*B*) nearly to confluence, then wounded with a pipette tip, and allowed to heal for 3 days. PAO1-GFP cells [10^7 colony-forming units (cfu)/ml] were added to filter or cover glass, and after 1 h, *P. aeruginosa* were washed. In addition, 5 μM fura 2-AM was added to apical and basolateral sides of filter so that cells could be visualized. Filter or cover glass was then mounted in microscope chamber for observation of cells. *Aa*: fluorescence image of PAO1-GFP cells. *Ab*: merged overlay of PAO1-GFP cells (bright white) on filter-grown, fura 2-loaded Calu-3 cells. PAO1-GFP cells bound to free edges of Calu-3 cells that had not completely covered the filter. *Ba*: fluorescence image of PAO1-GFP cells that were bound to cover glass-grown Calu-3 cells. *Bb*: fluorescence image of PAO1-GFP was inverted (i.e., to black) to improve contrast and overlaid on bright-field Nomarski image of cover glass-grown Calu-3 monolayers to create merged image. *P. aeruginosa* bound to Calu-3 cells at free edges of monolayer but not in confluent region of Calu-3 monolayer.
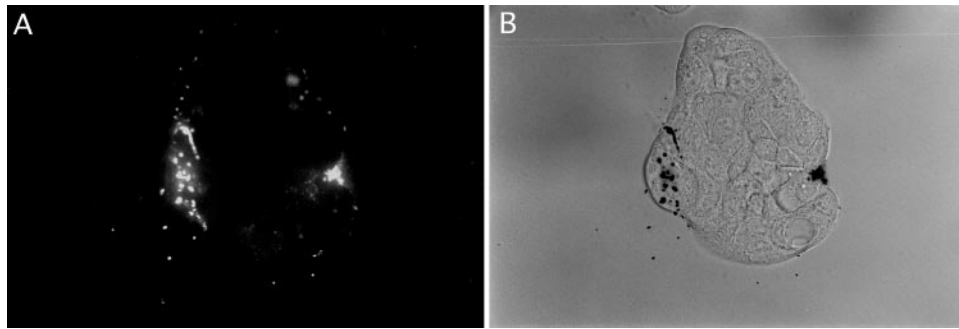
Fig. 2. PAO1-GFP cells bound to perimeters of Calu-3 islands and around holes in monolayers grown on cover glass. PAO1-GFP cells (10^7 cfu/ml) were added to Calu-3 cells grown as islands on cover glasses, and after 1 h, *P. aeruginosa* were washed off to eliminate loosely bound bacteria. Propidium iodide (PI; 1 μM) was added to solution to identify dead Calu-3 cells. Nomarski images of epithelial cells were merged with fluorescence images of bacteria. *A*: PAO1-GFP cells (bright white spots) fluorescence image. *B*: bacterial fluorescence was inverted (i.e., black) and merged with Nomarski image of Calu-3 island to show heterogeneous binding of *P. aeruginosa* to cells along free edge.

sections is shown in Fig. 4, *Aa–Ad*, where it can be seen that PAO1-GFP cells bound to the glass and to the basal and lateral regions of the cells adjacent to the free edge (Fig. 4, *Ac* and *Ad*). Even in sections in which a few PAO1-GFP cells were present in the topmost confocal sections, the bacteria appeared to bind to the lateral regions of cells that had exposed free edges (Fig. 4, *Aa*

Table 1. *PAO1-GFP binding along free edges of islands and wounds and to apical and basal membranes of Calu-3 cells*

Conditions	*n*	Average ± SD	Range
PAO1-GFP, μm from free edge			
Island	6	11 ± 4	2–40
Hole	5	17 ± 6	5–35
Wounds			
Dead cell	13	26 ± 13	10–70
Intact cell	15	29 ± 18	3–70
PAO1-GFP number			
Island			
Apical	6	2 ± 2	0–5
Basal	6	43 ± 23	32–74
Wound			
Apical	6	3 ± 2	0–6
Basal	6	54 ± 27	19–88

n, No. of experiments. Calu-3 cells were grown as islands or confluent monolayers that were wounded and then allowed to heal for 2–24 h. *Pseudomonas aeruginosa* strain O1 expressing green fluorescent protein [PAO1-GFP; 10^6 to 10^8 colony-forming units (cfu/ml)] were added for 1 h and then washed 3 times to remove loosely adherent bacteria. Wide-field and confocal micrographs were used to measure linear distances that PAO1-GFP were found from random regions of free edges surrounding Calu-3 islands and adjacent to holes in monolayers, wounded monolayers, and dead cells in wounded monolayers in 2–9 different samples. Averages of these 2–9 different random regions were then averaged to obtain an average distance ± SD (also including range) that PAO1-GFP were found away from free edges of islands, holes in monolayers, wounded monolayers containing dead cells, and wounded monolayers containing intact cells. Confocal images of the apicalmost section and basalmost regions of both islands and confluent monolayers that had been wounded and then allowed to heal were used to measure PAO1-GFP bound (after exposure of 10^6 to 10^7 cfu/ml for 1 h followed by 3 washes to eliminate loosely adherent bacteria) to apical and basal surfaces of Calu-3 cells. Bound PAO1-GFP were defined as those bacteria that were found within boundaries of cell.

and *Ab*). There was little or no binding of PAO1-GFP cells to the apical membranes of Calu-3 cells (Fig. 4*Ad*). Individual PAO1-GFP cells were counted in confocal images from the apicalmost and basalmost regions of islands like those shown in Fig. 4. We detected an average of only two PAO1-GFP cells at the apicalmost aspects of the islands (Table 1). In contrast, there was an average of 43 PAO1-GFP cells in the basalmost sections of the same islands (Table 1), all within 40 μm of a free edge (Table 1).

We also examined PAO1-GFP binding to Calu-3 monolayers that had been mechanically damaged, allowed to heal for 2–24 h, and then exposed to 10^6 to 10^8 cfu/ml of PAO1-GFP for 1 h (rather than the 1–3 days as in other experiments) before unbound *P. aeruginosa* was washed off and polarity of *P. aeruginosa* adherence was monitored. Dead cells (PI-positive nuclei) were found only along some wounds (presumably because dead cells had been sloughed from the monolayer during the healing time), whereas other regions had one or several dead epithelial cells lining the wound. PAO1-GFP cells always bound to dead cells and their undamaged nearest neighbors but more randomly to undamaged cells along the wound, similar to the binding of PAO1-GFP cells along wounded then healed monolayers that exhibited no dead cells. Confocal images showed that PAO1-GFP cells bound to basal and lateral membranes of Calu-3 cells that were adjacent to the wound (Fig. 4, *Bc* and *Bd*), but there was little or no binding to the apical membranes (Fig. 4, *Ba* and *Bb*). We detected an average of 3 PAO1-GFP cells at the apicalmost aspects of the monolayers. In contrast, there was an average of 54 PAO1-GFP cells in the basalmost sections of the same epithelial monolayers (Table 1), all within 70 μm of the free edges (Table 1).

There was somewhat more extensive PAO1-GFP binding along wounds or along free edges containing dead cells than at the free edges of unwounded islands: comparisons of monolayers that had been wounded with those of unwounded islands showed that PAO1-GFP cells were found farther from the free edge in the wounded epithelia than in the unwounded islands. As mentioned above, PAO1-GFP was found an average of
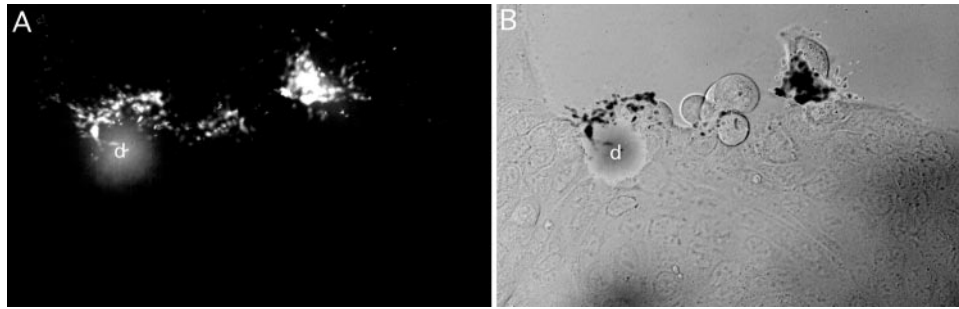
Fig. 3. PAO1-GFP cells bound to both dead and live cells at free edge of Calu-3 monolayer grown on cover glass. PAO1-GFP cells (10^7 cfu/ml) was added to Calu-3 cells grown to confluence on cover glasses, and after 1 h, *P. aeruginosa* were washed off to eliminate loosely bound bacteria. PI (1 μM) was added to solution to identify dead Calu-3 cells. *A*: fluorescence image showing both PAO1-GFP- and PI-stained nucleus (d) of dead Calu-3 cell. *B*: Nomarski image of Calu-3 cells was merged with inverted fluorescence image of bacteria (i.e., black to increase contrast) and PI-stained nucleus (d) from dead Calu-3 cell. PAO1-GFP bound both along free edge of otherwise confluent monolayer and to cells near dead cell. Because this preparation had not been mechanically damaged, this dead Calu-3 cell was present spontaneously.

11 μm from the free edge of the island (Table 1). Similar measurements on monolayers that had been wounded and then allowed to heal showed that PAO1-GFP cells were found an average of 29 μm from the edges of cell islands (Table 1), and there were no PAO1-GFP cells bound to regions farther than 70 μm from the free edges of the monolayers. PAO1-GFP cells were found an average of 26 μm from dead cells at the edges of monolayers and no farther than 70 μm from the free edge (Table 1). Therefore, PAO1-GFP cells were found closer to a free edge of either undamaged islands or holes (within 11–17 μm) and farther away from free edges of mechanically damaged monolayers (within 26–29 μm; Table 1).

An implication of the data to this point was that binding of *P. aeruginosa* to the basolateral membranes of cultured Calu-3 cells in confluent areas was prevented because *P. aeruginosa* could not migrate past the tight junctions. We tested whether confluent monolayers of primary, cultured bovine tracheal epithelial cells behaved similarly. Cells were grown to confluence on filters with an air-water interface and $R_t > 1,000$ $\Omega \cdot cm^2$. We then added 200 μl of Ringer solution containing $1–5 \times 10^7$ cfu/ml of PAO1-GFP and 10 μM fura 2-AM to the apical side for 1 h and washed the surface three times. The filters were then cut from the plastic support and placed in the chamber. As shown in Fig. 5, the confluent monolayers bound few bacteria. In 18 different randomly selected fields (3 different filters), we observed an average of 4 ± 3 *P. aeruginosa* bound/field of 300–500 epithelial cells.

PAO1-GFP binding to low R_t monolayers: Calu-3 monolayers in Ca-free solution and CFT1 monolayers. We tested whether tight junctions were limiting access of *P. aeruginosa* to critical basolateral binding sites using two approaches. First, Calu-3 cells were treated with a 1 mM EGTA-containing, Ca-free solution for 30 min (to open tight junctions) and then switched to a normal Ca-containing solution containing 10^7 cfu/ml of PAO1-GFP for 1 h. This treatment of Calu-3 cells grown on filters caused R_t to decrease from 1,000–2,500 to 0 $\Omega \cdot cm^2$, consistent with the idea that the tight junctions

had been disrupted. Cells were finally washed three times with normal Ringer solution to remove loosely adherent bacteria. After this treatment, PAO1-GFP cells bound to many, but not all, regions of the confluent monolayer that would normally have excluded *P. aeruginosa* (Fig. 6). The "patchy" binding of PAO1-GFP likely indicated the regions where EGTA was disrupting the tight junctions. The regions of the Calu-3 monolayers that bound PAO1-GFP cells often correlated with regions of the Calu-3 monolayers that appeared to have lifted off the cover glass but were still confluent.

The second general approach was to perform binding experiments on confluent CFT1 cell monolayers, a low R_t (100–200 $\Omega \cdot cm^2$), CFTR-expressing, tracheal-derived cell line. Ringer solution containing 10^7 cfu/ml of PAO1-GFP was placed on the apical surface, and after 1 h, the monolayers were washed three times to remove loosely adherent bacteria. The filter was then cut from the plastic cup and mounted in the chamber. In sharp contrast to the results obtained with Calu-3 cells, many PAO1-GFP cells bound to confluent regions of the CFT1 monolayer, particularly to the junctional regions between adjacent cells. Similar results were obtained when CFT1 cells were grown on cover glasses where it was possible to compare PAO1-GFP binding to cellular morphology. A typical example is shown in Fig. 7. These experiments showed that, unlike Calu-3 and bovine tracheal epithelial cells, PAO1-GFP cells bound similarly to the confluent regions of CFT1 cells that had been grown on either filters or cover glasses and also that there was apparently preferential binding of bacteria to the junctions compared with that to the cells.

We quantitated cellular and junctional binding sites by moving the microscope stage to random regions of the monolayer where individual epithelial cells could be easily observed. Then we collected a fluorescence image of PAO1-GFP cells that were bound in the same region. Fluorescence and bright-field images were overlaid, and PAO1-GFP cells that had bound to cells versus tight junctions were counted. In some cases (<10%), it was impossible to determine whether bacteria were
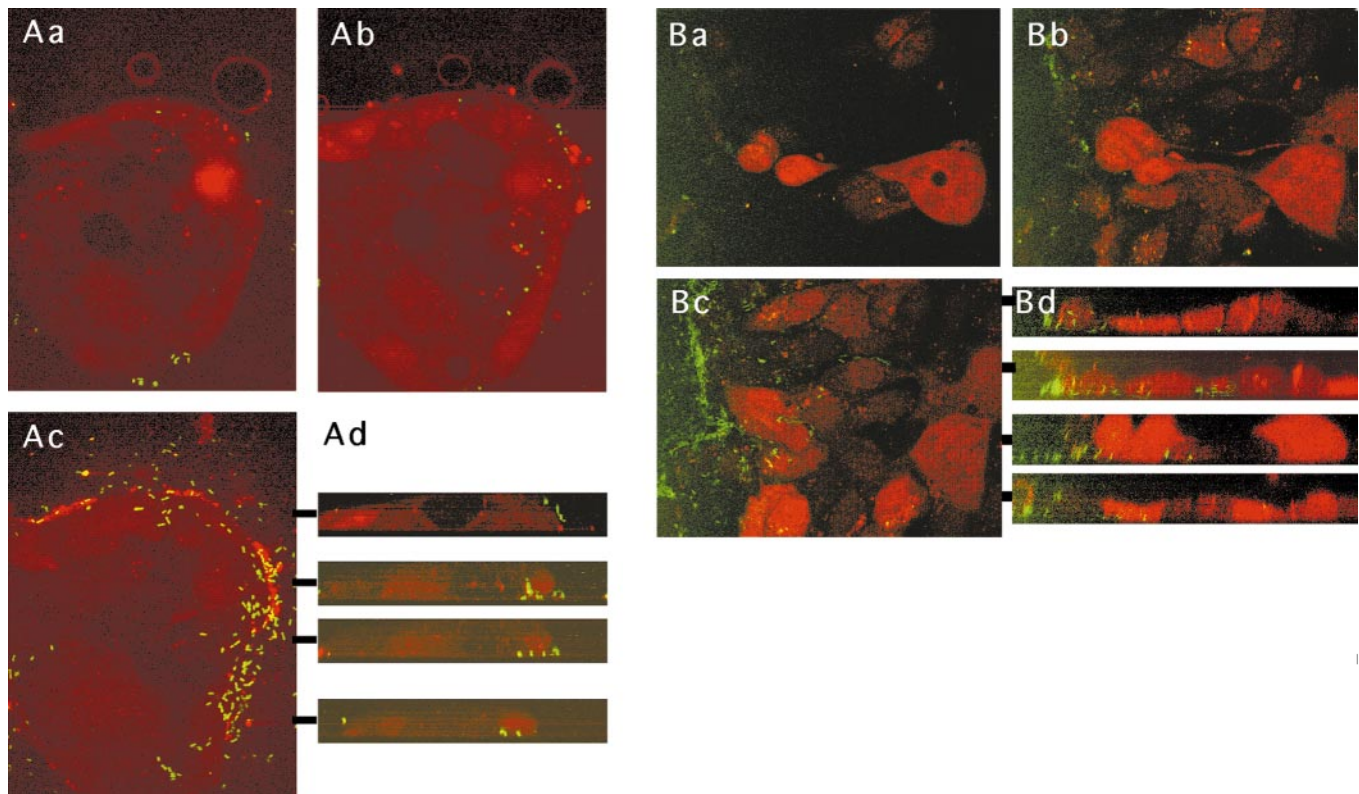
Fig. 4. Confocal sections of Calu-3 cells exposed to PAO1-GFP. *A*: PAO1-GFP cells bound to basal and lateral sides of cells near free edges of Calu-3 island. Calu-3 cells grown as islands on a cover glass were loaded with fura red, and 5×10^7 cfu/ml were added for 1 h. Cells were then washed with bacteria-free solution to remove loosely adherent *P. aeruginosa*, mounted in chamber, and examined with confocal microscope. Sections (0.5 µm) were stored and then displayed in 2.5-µm composite sections. *Aa*: section through topmost portion of island. *Ab*: section from middle portion of cell. *Ac*: section from bottom of cell. Note that majority of PAO1-GFP binding occurred in this bottommost section. *Ad*: 4 Z-sections were reconstructed from regions of monolayer shown by dark bars that connect to bottommost 2.5-µm section. These Z-sections emphasized binding of PAO1-GFP to basal and lateral surfaces of Calu-3 cells adjacent to free edge of island and lack of binding to apical membranes except at free edge of monolayer. *B*: confluent Calu-3 cells that had been mechanically wounded had PAO1-GFP cells bound only to basal and lateral sides of cells near free edges of wound. Calu-3 cells grown to confluence on a cover glass were loaded with fura red, mechanically wounded with a needle, and then allowed to heal for 1 h. PAO1-GFP cells (5×10^7 cfu/ml) were added to cells for 1 h. Cells were then washed with bacteria-free solution containing 1 µM PI (to identify dead cells) and then mounted in chamber and examined with confocal microscope. Sections (0.5 µm) were stored and then displayed in 2.5-µm composite sections similar to those in Fig. 2*A*. Topmost (*Ba*) and middle (*Bb*) sections showed little or no binding of PAO1-GFP. Bottommost section (*Bc*) showed extensive binding of PAO1-GFP, and PAO1-GFP cells were found farther from free edge in these wounded monolayers compared with island in Fig. 2*A*. Z-sections (*Bd*) were reconstructed from regions of monolayer shown by dark bars that connect to bottommost 2.5-µm section. Z-sections showed binding of PAO1-GFP to basal and lateral surfaces of Calu-3 cells near free edge of wound, but there was little PAO1-GFP binding to apical membranes.

binding cellular or junctional regions, and these bacteria were ignored. On average, when 10^7 cfu/ml of PAO1-GFP were used for binding, there were 20 ± 8 bacteria bound to ~200 cells in each field (89 images from 9 monolayers, 5 different cultures). Thus there was more binding of PAO1-GFP to CFT1 cells compared with that to bovine monolayers and Calu-3 cell monolayers. In the same experiments, PAO1-GFP appeared to bind preferentially to the regions between adjoining cells: an average of 14 ± 7 bacteria bound to this intercellular (junctional) region, whereas 4 ± 2 bacteria bound to cells in any one field (~200 cells/field of view). Thus, in CFT1 cells, there was a >3-fold preference for binding to regions just between adjacent cells compared with that in other portions of the cell. Similar

results were obtained with JME monolayers, a low R_t (10–100 $\Omega \cdot cm^2$) ΔF508 CFTR nasal epithelium.

Cytotoxic effects of PA6206 on high R_t Calu-3 monolayers required direct interaction between bacteria and basolateral membranes of epithelial cells. Cellular patterns of binding and cytotoxicity of PA6206 (response to 10^8 cfu/ml) on Calu-3 cells were investigated in cells grown both on filters and cover glasses. When 10^6 to 10^8 cfu/ml of PA6206 were added to the apical surfaces of these monolayers, R_t remained stable and then decreased rapidly (Fig. 8). Cytotoxicity (i.e., PI uptake) occurred only at the extreme periphery of these confluent monolayers, in regions adjacent to the edge of the plastic (data not shown). This effect was difficult to quantitate because it was impossible to determine
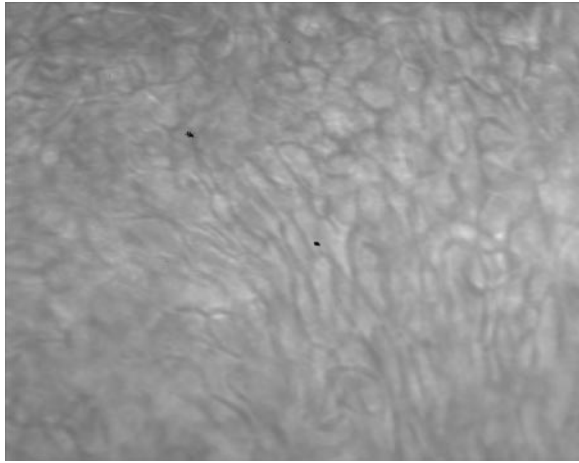
Fig. 5. Few PAO1-GFP cells bound to confluent primary cultured bovine tracheal epithelial cell monolayers. PAO1-GFP cells (2×10^7 cfu/ml) and fura 2-AM (10 µM) were added to apical side of monolayers grown to confluence, with $R_t > 1,000$ $\Omega \cdot$cm^2. Bacteria and dye were washed out, and filter was cut from filter cup and mounted on stage of microscope. Fluorescence image of the 2 bacteria was inverted and overlaid on fura 2 fluorescence of cells (~500 cells) to show cellular binding of *P. aeruginosa* (small black dots).

which cells were growing on the filter and which were growing up the plastic sides. We therefore performed experiments similar to those used to investigate PAO1-GFP binding. Calu-3 cells were grown to confluence and then wounded and allowed to heal for 3 days. FITC-labeled PA6206 cells (10^7 cfu/ml) were added to the apical surface for 1 h and then washed three times to remove loosely adherent bacteria. The cells were left in this configuration for an additional 2 h, which control experiments showed allowed sufficient time for cytotoxic reactions just to have begun. One micromolar PI was added to the solution to stain the nuclei of dead cells. As shown in Fig. 9, PA6206 cells, like PAO1-GFP cells, bound at the free edge of the monolayer, and cytotoxicity was initiated at the free edge where bacterial binding was occurring, not in confluent regions of the monolayer.

Longer-term experiments on random regions of Calu-3 cells with exposed free edges on either cover glasses or filters showed that cytotoxicity was dose dependent (Fig. 10) and occurred after ~2 h, first at the free edge of the epithelium, and was followed by further killing of epithelial cells inward from the free edge toward the confluent region of the monolayer (Fig. 11). Unlike the results obtained on low R_t MDCK cells (17), cytotoxicity was never initiated in confluent portions of the monolayers. Similar results were obtained with PA103 (data not shown). Thus cytotoxicity by both PA6206 and PA103 appeared to require that *P. aeruginosa* have access to the basolateral membranes of Calu-3 cells.

Experiments to test directly whether PA6206-induced cytotoxicity occurred only when *P. aeruginosa* actually contacted the basolateral surfaces of Calu-3 cells were performed by adding PA6206 to either the apical or basolateral surface of Calu-3 cells grown to confluence ($R_t > 1,000$ $\Omega \cdot$cm^2) on filters with 0.45-µm (too small to permit PA6206 access) or 1.0-µm (large enough to permit PA6206 access) pores. When 10^8 cfu/ml of PA6206 were added to the apical surfaces of cells grown on either 0.45- or 1.0-µm-pore filters, cytotoxicity occurred only along the free edges of the monolayers (Fig. 11, *A* and *B*). There was no cytotoxicity in confluent regions. Thus the addition of PA6206 to the apical side of Calu-3 cells grown on 0.45- or 1.0-µm-pore filters elicited the same pattern of cytotoxicity as that exhibited by Calu-3 cells grown on cover glasses. These results showed that apical addition of bacteria elicited cytotoxicity only along the free edges of Calu-3 islands.

In contrast, addition of PA6206 to the basal surface of cells grown on 0.45-µm-pore filters elicited no cytotoxicity along the wound edge (Fig. 11*C*). This showed that small-pore filters prevented PA6206 from eliciting cytotoxicity. In contrast, when PA6206 cells were added to the basal side of Calu-3 monolayers grown on 1.0-µm-pore filters, there was extensive, random damage throughout the monolayer of Calu-3 cells (Fig. 11*D*). Addition of PA6206 to the basal surface of confluent monolayers had no effect on either R_t (data not shown) or cytotoxicity when cells were grown on 0.45-µm-pore filters (Fig. 11*E*), whereas at the same time, *P. aeruginosa* on the basal side of confluent monolayers of Calu-3
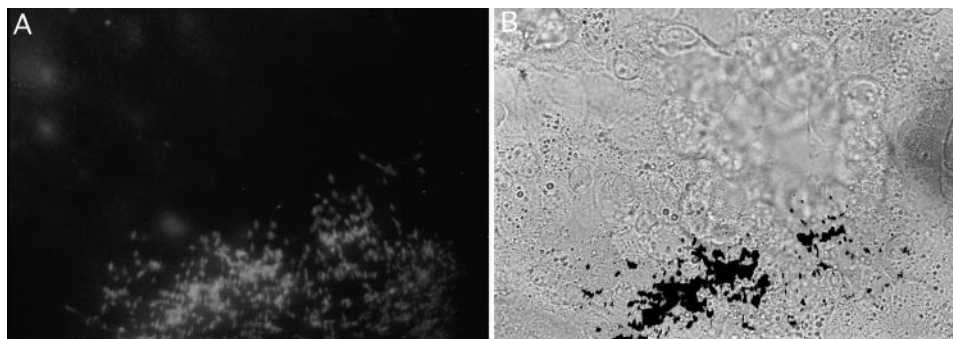

Fig. 6. Ca-free treatment of confluent monolayers of Calu-3 cells led to PAO1-GFP binding to cells that previously excluded bacteria. Calu-3 cells were grown to confluence on cover glasses and then treated for 30 min with Ca-free EGTA (1 mM) solution. Cells were returned to Ca-containing solution containing PAO1-GFP cells (10^7 cfu/ml) for 60 min and then washed with fresh Ca-containing Ringer solution. Bacterial fluorescence (*A*) was overlaid on Nomarski micrograph of epithelial cells to generate merged image (*B*) showing PAO1-GFP cells (inverted to black to improve contrast) bound to many cells within confluent region.

Fig. 7. PAO1-GFP bound throughout confluent regions of low R_t CFT1 monolayers. CFT1 cells were grown to confluence on cover glasses. PAO1-GFP cells (10^7 cfu/ml) were added to CFT1 cells for 1 h, and bacteria were then washed. Fluorescence image of PAO1-GFP cells (*A*) was inverted (black) and overlaid on Nomarski image to yield merged image (*B*) showing that *P. aeruginosa* bound prominently to junctional regions between adjacent cells as well as to cells in confluent regions of monolayer.
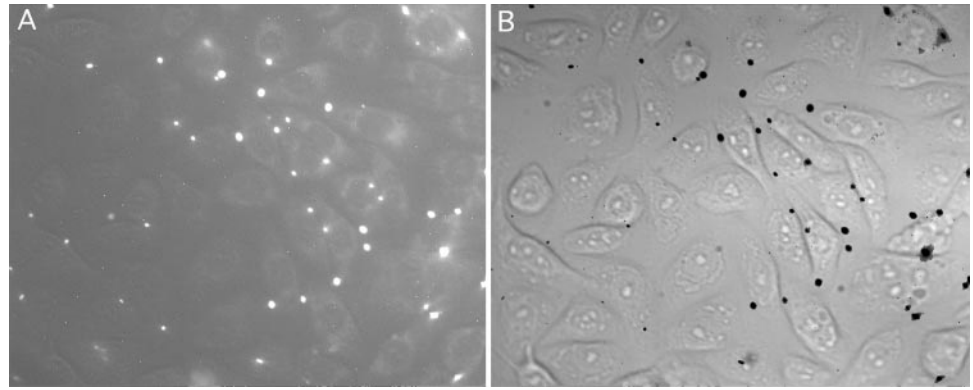
cells grown on 1.0-µm-pore filters elicited random and extensive epithelial cell killing (Fig. 11*F*).

Role of junctional tightness on P. aeruginosa-induced cytotoxicity: effects of PA6206 on low R_t CFT1 cell monolayers. CFT1 cells were used to test the apparent role of tight junctions on the pattern of PA6206-induced cytotoxicity. Because previous experiments showed that *P. aeruginosa* binding to CFT1 cells was similar whether they were grown on filters or coverslips, we utilized cover glass-grown CFT1 cells to facilitate microscopic observations. CFT1 grown on cover glasses were exposed to a solution containing 5 µM fura 2-AM and 10^7 cfu/ml of FITC-labeled PA6206. After 1 h, the cells were washed three times to remove the dye and loosely adherent bacteria. The cells were left for an additional 0.5–1 h, which control experiments showed was sufficient time just to begin expression of cytotoxicity. One micromolar PI was added to the cells, which were then examined. Typical images are shown in Fig. 12. Several aspects should be noted. PA6206 cells, like PAO1-GFP cells, bound frequently to regions between adjacent epithelial cells throughout the confluent monolayer. Also, nuclei throughout the confluent CFT1 monolayer were stained with PI, not just at the free edges of the monolayer as in Calu-3 cells. In addition, many PA6206-treated epithelial cells throughout the monolayer lost fura 2 even though they had not yet become permeable to PI. Control experiments showed that CFT1 cells that had not been exposed to PA6206 were stained uniformly by fura 2 and did not take up PI. Thus PA6206 bound and elicited cytotoxicity to CFT1 cells throughout the monolayer, and there appeared to be preferential binding of PA6206 to junctional regions between cells. Time-course experiments showed that, compared with the free-edge type of killing exhibited by PA6206 on Calu-3 cells, the apparently random PA6206-induced killing of CFT1 cells occurred after a shorter delay (15–20 vs. 120 min) and once cytotoxicity occurred more quickly (18 Calu-3 vs. 120 CFT1 cells/h with 10^8 cfu/ml of PA6206).

DISCUSSION

Tight junctions of high R_t tracheal epithelial cells prevent airway disease by restricting access of bacteria to basolateral membranes. Fleiszig et al. (10) previously noted that there was an inverse correlation between R_t

of different epithelial cell types and susceptibility to *P. aeruginosa* binding and cytotoxicity and also that all epithelial cell types were more susceptible to the bacteria once tight junctions had been disrupted. The present results are consistent with these findings and have extended them in a number of ways. *P. aeruginosa* both bound and exerted cytotoxicity heterogeneously, but selectively, to high R_t Calu-3 cells by interacting with basolateral membranes of cells that were positioned near a free edge (within a few cell diameters). *P. aeruginosa* were always located within 2–70 µm of the free edges of Calu-3 monolayers, and cytotoxicity was initiated from these free edges where *P. aeruginosa* had access to the basolateral membranes. There was little or no detectable binding of apically added *P. aeruginosa* (either PAO1 or PA6206) in confluent Calu-3 or bovine tracheal monolayers in regions that were >70 µm from a free edge, and cytotoxicity was initiated in confluent regions only when holes or other epithelial discontinuities were present. Confocal microscopy showed that there were ~25 times as many PAO1
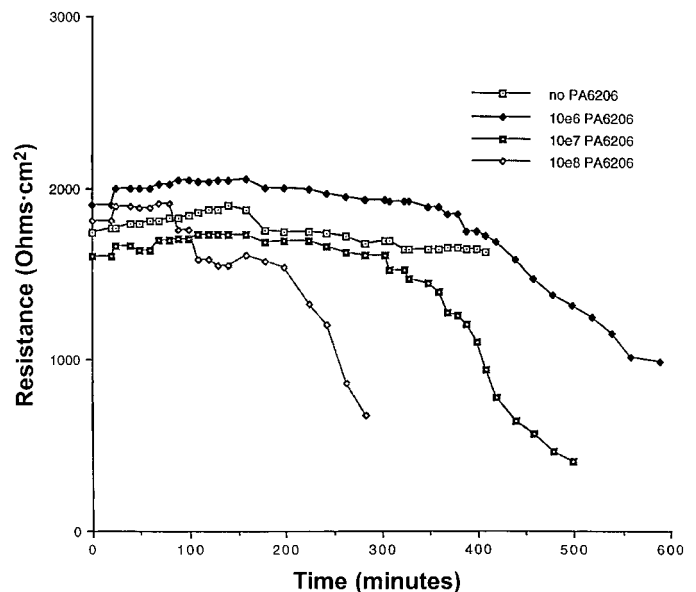

Fig. 8. Effects of apically added PA strain 6206 (PA6206) on R_t of confluent Calu-3 monolayers. PA6206 (10^6, 10^7, and 10^8 cfu/ml) were added to apical surface of confluent Calu-3 monolayers, and R_t was measured at times shown.
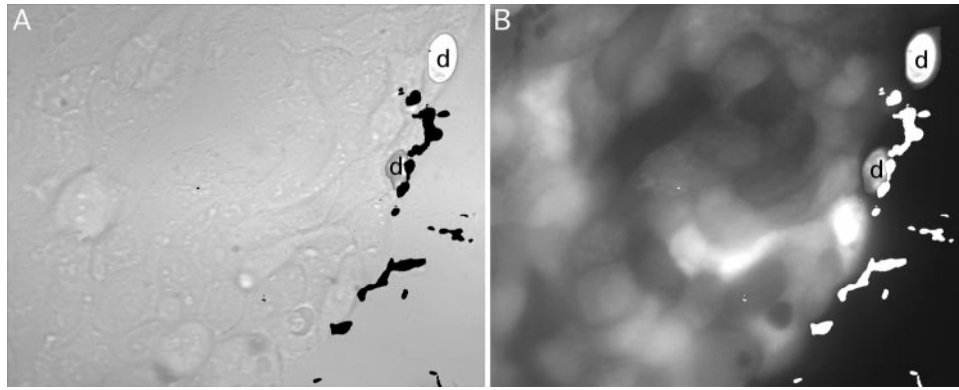
Fig. 9. PA6206 binding and initiation of cytotoxicity at free edge of Calu-3 monolayer grown on filter. PA6206 cells (5×10^7 cfu/ml) that had been FITC labeled plus 5 μM fura 2-AM were added to a Calu-3 monolayer that had been grown to confluence, wounded, and then allowed to heal for 3 days. After 1 h, cells were washed, and 1 μM PI was added to monolayer, which was left for an additional 1 h. Cover glass was then washed again and mounted in chamber for observation. *A*: fluorescence from PA6206 was inverted (i.e., black) and overlaid along with PI-stained nuclei (d) of dead cells on Nomarski bright-field image to show cellular pattern of bacterial binding along free edge of monolayer. *B*: fluorescence from PA6206 (shown as bright white to improve contrast) was overlaid on fluorescence of fura 2-stained cells (dimmer white monolayer) and PI-stained nuclei (d) to show relationships among live and dead Calu-3 cells and bound PA6206. Note that *P. aeruginosa* were bound to both epithelial cells that had taken up PI and lost their fura 2 and cells that retained fura 2 and excluded PI.

cells bound to the basal surfaces of the same Calu-3 cells that bound only very small numbers of *P. aeruginosa* at the apical surface. PAO1 cells were detected farther from free edges of wounded monolayers (26–29 μm) compared with Calu-3 islands that had not been wounded (11–17 μm).

It might be argued that the binding studies with PAO1-GFP were artifactual because PAO1-GFP bound to abundant basolateral sites with low affinity and that the methods were insufficiently sensitive to observe PAO1-GFP binding to more critical high-affinity but less abundant sites on the apical surface. However, cytotoxicity to high R_t Calu-3 cells at all doses of

PA6206 (and PA103) began only when bacteria had access to exposed basolateral membranes, i.e., cells with a free edge on the periphery of islands or adjacent to small holes or healing areas of mechanically damaged epithelium. This implied that, similar to the binding of PAO1, the critical receptors involved in the susceptibility to cytotoxicity were at the basolateral, not at the apical, sides of Calu-3 cells. Also, apically added *P. aeruginosa* bound to Calu-3 cells in confluent monolayers in which the basolateral membranes had become exposed to the luminal solution by EGTA treatment to open tight junctions.

PA6206-induced cytotoxicity required direct contact of P. aeruginosa with the basolateral membranes of Calu-3 cells. Unlike low R_t CFT1 and MDCK cells (1), *P. aeruginosa* did not induce cytotoxicity when added to the apical side of high R_t Calu-3 cells unless *P. aeruginosa* had access to the basolateral membrane at free edges of wounds or holes in the monolayer. *P. aeruginosa* did not elicit cytotoxicity from the basolateral side if the filters had pores that were too small to allow access of *P. aeruginosa* to the Calu-3 cells, indicating that secreted factors were insufficient in themselves to elicit cytotoxicity. Instead, *P. aeruginosa* exerted cytotoxicity to Calu-3 cells only when they had access through the large-pore filters to the basolateral membrane. Our results therefore showed for the first time that *P. aeruginosa*-induced cytotoxicity required direct contact of bacteria with basolateral membranes of airway epithelial cells, a finding consistent with recent experiments (9) showing that ExoU, which is likely secreted by a type III secretion mechanism, is critical for *P. aeruginosa*-induced cytotoxicity. The use of large-pore filters will provide a useful experimental approach for testing the specificity of basolateral *P. aeruginosa*-epithelial cell interactions and cytotoxicity in future experiments.
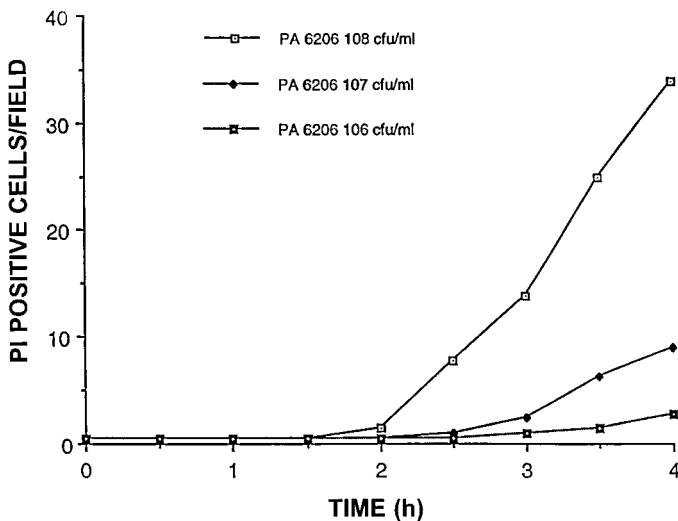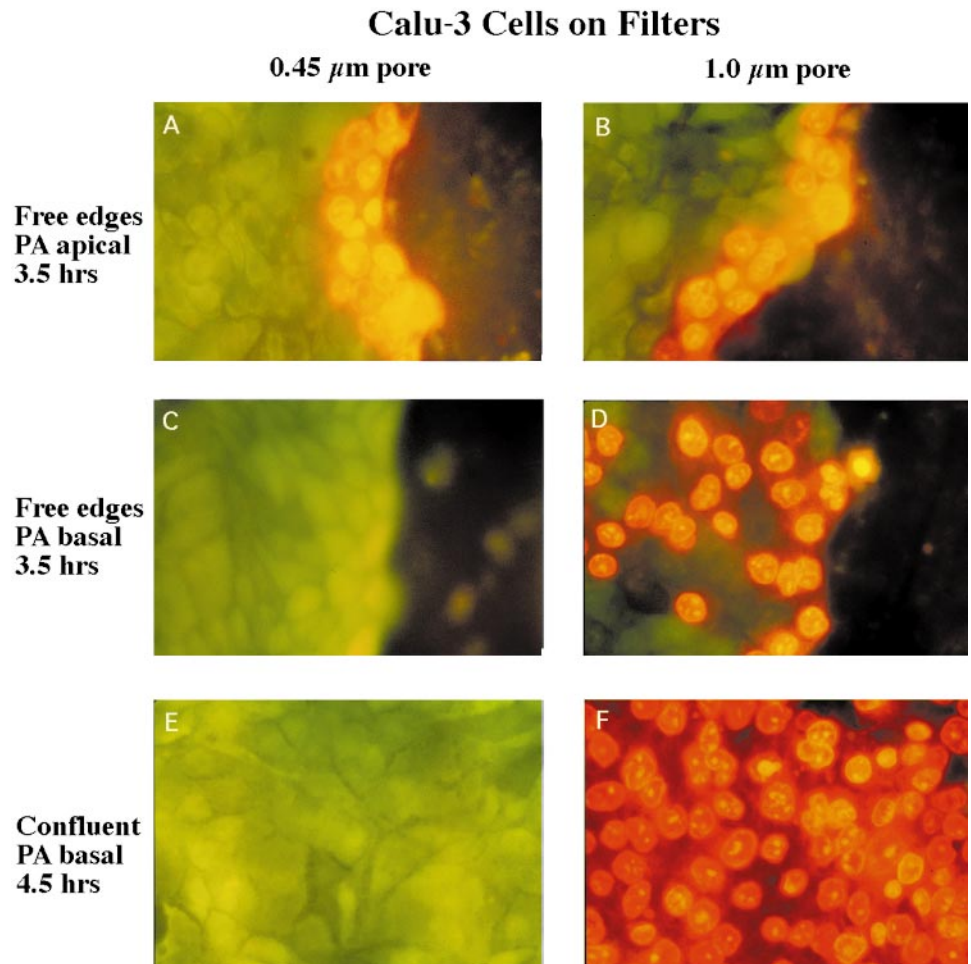

Fig. 10. Dose dependence of PA6206-induced killing of Calu-3 cells vs. time. Calu-3 cells were grown as islands, and 10^6, 10^7, or 10^8 cfu/ml were added in presence of 1–10 μM PI. At times shown, PI-positive nuclei were counted in 10 random edges (where cytotoxicity occurred) of islands. Values are averages from these 10 random edges. Increasing doses of PA6206 caused increasing amount of cytotoxicity. Results are typical of 3 other experiments.

Fig. 11. PA6206 required direct contact with Calu-3 cells to elicit cytotoxicity. Calu-3 cells were grown to confluence on 0.45-µm-pore (*A, C,* and *E*) or 1.0-µm-pore (*B, D,* and *F*) filters and then left in a confluent state or mechanically damaged and allowed to heal for 24 h. Cells were loaded with 2′,7′-bis(2-carboxyethyl)-5(6)-carboxyfluorescein (BCECF; green fluorescence), and then 10^8 cfu/ml were added to apical (*A* and *B*) or basolateral (*C–F*) surfaces of filters. PI (1 µM) was added to solutions to stain nuclei of dead cells (red). When PA6206 cells were added to apical side of cells grown on either 0.45-µm-pore (*A*) or 1.0-µm-pore (*B*) filters, cytotoxicity (as shown by red-orange PI staining of nuclei) occurred only along free edges of wounds after 3.5 h. There was similar but more extensive cytotoxicity after 4.5 and 5.5 h along free edges of monolayers (data not shown). When PA6206 cells were added to basal sides of monolayers (*C–F*), there was no cytotoxicity to cells grown on 0.45-µm-pore filters after 3.5 h (*C*) but widespread and random (i.e., no preference for wound edge) cytotoxicity to cells grown on 1.0-µm-pore filters (*D*). Note in *D* that PI-stained nuclei were intermingled with BCECF-loaded cells that did not take up PI, showing random nature of cytotoxicity. Similarly, addition of PA6206 for 4.5 h to basal surface of confluent monolayers elicited no cytotoxicity if cells were grown on 0.45-µm-pore filters (*E*) but extensive, random cytotoxicity to cells grown on 1.0-µm-pore filters (*F*).

Calu-3 Cells on Filters

0.45 µm pore   1.0 µm pore

Free edges PA apical 3.5 hrs

Free edges PA basal 3.5 hrs

Confluent PA basal 4.5 hrs

Low R_t CFT1 monolayers bound more P. aeruginosa and allowed random cytotoxicity throughout the confluent region of the monolayer compared with high R_t Calu-3 cells. Confluent, low R_t tracheal epithelial CFT1 monolayers bound about 25 times more *P. aeruginosa* than did confluent regions of the high R_t Calu-3 or primary bovine tracheal cell monolayers. CFT1 (and also low R_t JME) epithelial cells bound *P. aeruginosa* selectively in the regions between adjacent cells, indicating that binding sites may be localized to these regions (tight junctions?) of the cells. *P. aeruginosa* also bound, although three times less frequently, to cell membranes of CFT1 cells. Our methods did not provide enough resolution to determine whether *P. aeruginosa* were bound to the apical surfaces of junctions in the shallow furrows somewhat below the apical cell membranes that protruded slightly above the level of the junctions. It was also possible that the bacteria gained access in some way to the lateral intercellular space and were bound there. In any case, these experiments showed that *P. aeruginosa* binding to the low R_t CFT1 cells was very different from that exhibited by the high R_t Calu-3 cells.

We acknowledge that although the R_t of CFT1 monolayers was generally 100–200 $\Omega \cdot cm^2$ when grown on filters and results with filter- and cover glass-grown cells were similar, it was impossible to determine whether all the cells in the monolayers were completely polarized. However, our studies clearly showed that apically added *P. aeruginosa* bound very differently to the apical membranes of high and low R_t airway epithelial cells: *P. aeruginosa* bound only at the perimeters, near the edges of the filters, in confluent high R_t Calu-3 monolayers, whereas *P. aeruginosa* bound throughout the confluent monolayer of low R_t CFT1 cells. A corollary of our results is that comparisons of *P. aeruginosa* binding to epithelial cells will require using epithelia that are closely matched in terms of R_t. Further microscopy-based studies to determine whether different physiological states (e.g., different hormonal treatments) are associated with differences in *P. aeruginosa* binding to cell versus junctional regions of airway epithelial cells could provide insights into the interactions between *P. aeruginosa* and airway epithelial cells in both control and disease states.

In addition to differences in binding, *P. aeruginosa*-induced cytotoxicity occurred after a much shorter delay and faster and randomly throughout confluent CFT1 monolayers rather than only at the free edges of the Calu-3 monolayers. We observed many images of monolayers in which some cells had lost fura 2 and taken up PI, whereas other cells had only lost cytosolic fura 2 but had not yet taken up PI and still others had retained fura 2 and were impermeant to PI. One
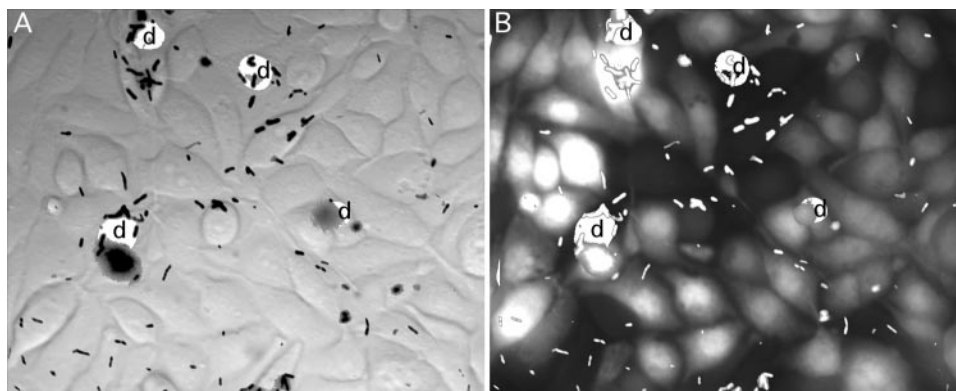
Fig. 12. Cellular pattern of PA6206 binding and cytotoxicity to CFT1 cells. CFT1 were grown on cover glass, and 10^7 cfu/ml of FITC-labeled PA6206 and 5 µM fura 2-AM were added and then washed off after 1 h. After an additional 1 h, 1 µM PI was added, and monolayer was examined. *A*: fluorescence of FITC-labeled PA6206 (shown as black dots to improve contrast) and PI-stained nuclei (d) of dead cells were overlaid on Nomarski image. *B*: fluorescence of FITC-labeled PA6206 (white to improve contrast) and PI-stained nuclei (d) of dead cells were overlaid on fura 2 fluorescence image to show patterns of PA6206 binding and cytotoxicity.

possible explanation was that cells were damaged in a time-dependent, graded fashion, first losing fura 2 and later becoming freely permeable to PI. In any case, the faster time course of cytotoxicity in low versus high R_t epithelia indicated that the delay between the time of *P. aeruginosa* addition and the initiation of cytotoxicity likely reflected in part the time required for *P. aeruginosa* to gain access to the critical sites, and these sites were more accessible in low versus high R_t airway epithelia. After binding, cytotoxicity seems to involve tyrosine kinase-coupled reactions (7), and the cells then appear to become leaky such that fura 2 is lost from the cells followed by the uptake of PI. Further microscopy-based time-course studies of *P. aeruginosa*-induced cytotoxicity may yield insights into the cellular reactions involved.

We observed similar patterns and amounts of *P. aeruginosa* binding and cytotoxicity to both CFT1 cells (which express CFTR) and JME cells (which do not), indicating that these processes did not depend on CFTR. Similar comments pertain to binding of *P. aeruginosa* to asialo-G_{M1} (32). Our studies instead emphasize the importance of junctional tightness in *P. aeruginosa* binding and cytotoxicity.

Binding of P. aeruginosa to Calu-3 cells was enhanced in mechanically damaged regions of the monolayer. PAO1 cells were found at larger distances from the free edges of wounded versus control Calu-3 islands and holes. However, PAO1 bound equally well to injured and healthy Calu-3 cells along wounds. This indicated that injured or dead Calu-3 cells did not specifically bind more *P. aeruginosa* than control, nondamaged cells in the same mechanically disturbed region of the monolayer, i.e., cells did not necessarily have to be injured to be susceptible to *P. aeruginosa* binding and sequelae. Thus mechanical disruption of the Calu-3 monolayer increased *P. aeruginosa* binding because bacteria had increased access to the basolateral membranes, not because dead cells bound more *P. aeruginosa* than live cells. It therefore seems likely that mechanical damage, likely including the "loosening" of

cell attachments to the underlying support and/or matrix near the wound, was responsible for the fact that PAO1 cells bound and/or migrated farther away from the free edge toward the intact, unwounded epithelium in mechanically damaged compared with control epithelial sheets. Thus our findings with Calu-3 cells suggested that the reason cell injury promotes adherence to and infection of the trachea (28, 29) is that the damage exposes the basolateral surfaces of the cells and that this, not cellular injury, increased susceptibility to *P. aeruginosa* binding of wounded tissues as proposed previously by Finck-Barbançon et al. (9).

Identity of P. aeruginosa binding sites on epithelial cells remains unknown. Although the specific binding sites for *P. aeruginosa* on epithelial cells remain unknown, several possibilities have emerged from these studies. Many PAO1 cells bound near the basal aspect of Calu-3 cells, so it seems possible that there is a role for the extracellular matrix or epithelial junctional proteins in binding. Based on the fact that *P. aeruginosa* bound preferentially to regions between adjacent CFT1 (and JME) cells and that there were images in which *P. aeruginosa* also bound to regions between adjacent Calu-3 cells, it seems possible that a junctional protein may also have been involved. Mistargeting of basolateral proteins to the apical sides of epithelial cells may also play a role in *P. aeruginosa*-induced pathogenesis (4, 11). In any case, the binding sites appear to be localized near regions between adjacent cells (at intercellular junctions?) in low R_t epithelial cells. In addition, for airway epithelia with $R_t > 1,000$ $\Omega \cdot cm^2$, apical *P. aeruginosa* did not bind or exert cytotoxicity. In contrast, the addition of PAO1 to the apical sides of intermediate R_t (200–500 $\Omega \cdot cm^2$) tracheal epithelial cells led to high levels of *P. aeruginosa* binding (up to 1 *P. aeruginosa*/epithelial cell) and dramatic changes in ion and fluid transport properties of the tissue (8), and we found that apical addition of *P. aeruginosa* to low R_t CFT1 and JME cells led to high-level binding and rapid cytotoxicity. The implication is that *P. aeruginosa* bound and exerted effects

from the apical surface of low ($20-100$ $\Omega \cdot cm^2$) and intermediate ($200-500$ $\Omega \cdot cm^2$) R_t but not of high R_t ($>1,000$ $\Omega \cdot cm^2$) airway epithelial cells.

REFERENCES

1. **Apodaca, G., M. Bomsel, R. Lindstedt, J. Engel, D. Frank, K. E. Mostov, and J. Wiener-Kronish.** Characterization of *Pseudomonas aeruginosa*-induced MDCK cell injury: glycosylation-defective host cells are resistant to bacterial killing. *Infect. Immun.* 63: 1541–1551, 1995.

2. **De Bentzmann, S., P. Roger, F. Dupuit, O. Bajolet-Laudinat, C. Fuchey, M. C. Plotkowski, and E. Puchelle.** Asialo GM1 is a receptor for *Pseudomonas aeruginosa* adherence to regenerating respiratory epithelial cells. *Infect. Immun.* 64: 1582–1588, 1996.

3. **De Bentzmann, S., P. Roger, and E. Puchelle.** *Pseudomonas aeruginosa* adherence to remodelling respiratory epithelium. *Eur. Respir. J.* 9: 2145–2150, 1996.

4. **De Boer, E. C., R. F. M. Bevers, K.-H. Kurth, and D. H. J. Schambert.** Double fluorescent flow cytometric assessment of bacterial internalization and binding by epithelial cells. *Cytometry* 25: 381–387, 1996.

5. **Bloemberg, G. V., G. A. O'Toole, B. J. Lugtenberg, and R. Kolter.** Green fluorescent protein as a marker for *Pseudomonas* spp. *Appl. Environ. Microbiol.* 63: 4534–4551, 1997.

6. **Drevets, D. A., and P. A. Campbell.** Macrophage phagocytosis: use of fluorescence microscopy to distinguish between extracellular and intracellular bacteria. *J. Immunol. Methods* 142: 31–38, 1991.

7. **Evans, D. J., D. W. Frank, V. Finck-Barbançon, C. Wu, and S. M. J. Fleiszig.** *Pseudomonas aeruginosa* invasion and cytotoxicity are independent events, both involving protein tyrosine kinase activity. *Infect. Immun.* 66: 1453–1459, 1998.

8. **Evans, D. J., P. S. Matsumoto, J. H. Widdicombe, C. Li-Yun, A. A. Maminishkis, and S. S. Miller.** *Pseudomonas aeruginosa* induces changes in fluid transport across airway surface epithelia. *Am. J. Physiol.* 275 (*Cell Physiol.* 44): C1284–C1290, 1998.

9. **Finck-Barbançon, V., J. Goranson, L. Zhu, T. Sawa, J. P. Wiener-Kronish, S. M. Fleiszig, C. Wu, L. Mende-Mueller, and D. W. Frank.** ExoU expression by *Pseudomonas aeruginosa* correlates with acute cytotoxicity and epithelial injury. *Mol. Microbiol.* 25: 547–557, 1997.

10. **Fleiszig, S. M., D. J. Evans, N. Do, V. Vallas, S. Shin, and K. E. Mostov.** Epithelial cell polarity affects susceptibility to *Pseudomonas aeruginosa* invasion and cytotoxicity. *Infect. Immun.* 65: 2861–2867, 1997.

11. **Fleiszig, S. M., V. Vallas, C. H. Jun, L. Mok, D. F. Balkovetz, M. G. Roth, and K. E. Mostov.** Susceptibility of epithelial cells to *Pseudomonas aeruginosa* invasion, and cytotoxicity is upregulated by hepatocyte growth factor. *Infect. Immun.* 66: 3443–3446, 1998.

12. **Fleiszig, S. M., J. P. Wiener-Kronish, H. Miyazaki, V. Vallas, K. E. Mostov, D. Kanada, T. Sawa, T. S. Yen, and D. W. Frank.** *Pseudomonas aeruginosa*-mediated cytotoxicity and inva-

13. sion correlate with distinct genotypes at the loci encoding exoenzyme S. *Infect. Immun.* 65: 579–586, 1997.

14. **Fleiszig, S. M. J., T. S. Zaidi, M. J. Preston, M. Grout, D. J. Evans, and G. B. Pier.** The relationship between cytotoxicity and epithelial cell invasion by corneal isolates of *Pseudomonas aeruginosa*. *Infect. Immun.* 64: 2288–2294, 1996.

15. **Gupta, S. K., R. S. Berk, S. Masinick, and L. D. Hazlett.** Pili and lipopolysaccharide of *Pseudomonas aeruginosa* bind to the glycolipid asialo GM1. *Infect. Immun.* 62: 4572–4579, 1994.

17. **Illek, B., H. Fischer, and T. E. Machen.** Alternate stimulation of apical CFTR by genistein in epithelia. *Am. J. Physiol.* 270 (*Cell Physiol.* 39): C265–C275, 1996.

18. **Illek, B., J. R. Yankaskas, and T. E. Machen.** cAMP and genistein stimulate HCO_3^- conductance through CFTR in human airway epithelia. *Am. J. Physiol.* 272 (*Lung Cell. Mol. Physiol.* 16): L752–L761, 1997.

19. **Imundo, L., J. Barasch, A. Prince, and Q. Al-Awqati.** Cystic fibrosis epithelial cells have a receptor for pathogenic bacteria on their apical surface. *Proc. Natl. Acad. Sci. USA* 92: 3019–3023, 1995.

20. **Kang, P. J., A. R. Hauser, G. Apodaca, S. M. Fleiszig, J. Wiener-Kronish, K. Mostov, and J. N. Engel.** Identification of *Pseudomonas aeruginosa* genes required for epithelial cell injury. *Mol. Microbiol.* 24: 1249–1262, 1997.

21. **Kondo, M., W. E. Finkbeiner, and J. H. Widdicombe.** Simple technique for culture of highly differentiated cells from dog tracheal epithelium. *Am. J. Physiol.* 261 (*Lung Cell. Mol. Physiol.* 5): L106–L117, 1991.

22. **Krivan, H. C., D. D. Roberts, and V. Ginsburg.** Many pulmonary pathogenic bacteria bind specifically to the carbohydrate sequence GalNAcβ1–4Gal found in some glycolipids. *Proc. Natl. Acad. Sci. USA* 85: 6157–6161, 1988.

24. **Olsen, J. C., L. G. Johnson, M. J. Stutts, B. Sarkadi, J. R. Sarkadi, J. R. Yankaskas, R. Swanstrom, and R. C. Boucher.** Correction of the apical membrane chloride channel defect in polarized cystic fibrosis airway epithelia following retroviral-mediated gene transfer. *Hum. Gene Ther.* 3: 253–266, 1992.

25. **Pier, G. B., M. Grout, and T. S. Zaidi.** Cystic fibrosis transmembrane conductance regulator is an epithelial cell receptor for clearance of *Pseudomonas aeruginosa* from the lung. *Proc. Natl. Acad. Sci. USA* 94: 12088–12093, 1997.

26. **Pier, G. B., M. Grout, T. S. Zaidi, and J. B. Goldberg.** How mutant CFTR may contribute to *Pseudomonas aeruginosa* infection in cystic fibrosis. *Am. J. Respir. Crit. Care Med.* 154: S175–S182, 1996.

27. **Pier, G. B., M. Grout, T. S. Zaidi, J. C. Olsen, L. G. Johnson, J. R. Yankaskas, and J. B. Goldberg.** Role of mutant CFTR in hypersusceptibility of cystic fibrosis patients to lung infections. *Science* 271: 64–67, 1996.

28. **Ramphal, R., M. T. McNiece, and F. D. Pollack.** Adherence of *Pseudomonas aeruginosa* to the injured cornea. A step in the pathogenesis of corneal infections. *Ann. Ophthalmol.* 100: 1956–1958, 1981.

29. **Ramphal, R., and M. Pyle.** Adherence of mucoid and nonmucoid *Pseudomonas aeruginosa* to acid-injured tracheal epithelium. *Infect. Immun.* 41: 345–351, 1983.

30. **Saiman, L., and A. Prince.** *Pseudomonas aeruginosa* pili bind to asialoGM1 which is on the surface of cystic fibrosis epithelial cells. *J. Clin. Invest.* 92: 1875–1880, 1993.

31. **Shen, B. Q., W. E. Finkbeiner, J. J. Wine, R. J. Mrsny, and J. H. Widdicombe.** Calu-3: a human airway epithelial cell line that shows cAMP-dependent Cl^- secretion. *Am. J. Physiol.* 266 (*Lung Cell. Mol. Physiol.* 10): L493–L501, 1994.

32. **Sheth, H. B., K. K. Lee, W. Y. Wong, G. Srivastava, O. Hindsgaul, R. S. Hodges, W. Paranchych, and R. T. Irvin.** The pili of *Pseudomonas aeruginosa* strains PAK and PAO bind specifically to the carbohydrate sequence β GalNAc(1–4) β Gal found in glycosphingolipids asialo-GM1 and asialo-GM2. *Mol. Microbiol.* 11: 715–723, 1994.

33. **Wu, R., J. Yankaskas, E. Cheng, M. R. Knowles, and R. C. Boucher.** Growth and differentiation of human nasal epithelial cells in culture: serum-free, hormone-supplemented medium and

proteoglycan synthesis. *Am. Rev. Respir. Dis.* 132: 311–320, 1985.

34. **Yahr, T. L., J. Goranson, and D. W. Frank.** Exoenzyme S of *Pseudomonas aeruginosa* is secreted by a type III pathway. *Mol. Microbiol.* 22: 991–1003, 1996.

35. **Yankaskas, J. R., J. E. Haizlip, M. Conrad, D. Koval, E. Lazarowski, A. M. Paradiso, C. A Rinehart, B. Sarkadi, R. Schlegel, and R. C. Boucher.** Papilloma virus immortalized tracheal epithelial cells retain a well-differentiated phenotype. *Am. J. Physiol.* 264 (*Cell Physiol.* 33): C1219–C1230, 1993.

36. **Zar, H., L. Saiman, L. Quittell, and A. Prince.** Binding of *Pseudomonas aeruginosa* to respiratory epithelial cells from patients with various mutations in the cystic fibrosis transmembrane regulator. *J. Pediatr.* 126: 230–233, 1995.

37. **Zoutman, D. E., W. C. Hulbert, B. L. Pasloske, A. M. Joffe, K. Volpel, M. K. Trebilcock, and W. Paranchych.** The role of polar pili in the adherence of *Pseudomonas aeruginosa* to injured canine tracheal cells: a semiquantitative morphologic study. *Scanning Microsc.* 5: 109–126, 1991.